Studies of valence shell photoionization of Cl2

M. Braunstein and V. McKoy

Citation: The Journal of Chemical Physics **92**, 4887 (1990); doi: 10.1063/1.457705
View online: http://dx.doi.org/10.1063/1.457705
View Table of Contents: http://scitation.aip.org/content/aip/journal/jcp/92/8?ver=pdfcov
Published by the AIP Publishing

Studies of valence shell photoionization of Cl_2

M. Braunstein and V. McKoy
Arthur Amos Noyes Laboratory of Chemical Physics,[a] *California Institute of Technology, Pasadena, California 91125*

(Received 16 October 1989; accepted 4 January 1990)

We report photoionization cross sections and photoelectron angular distributions for the $5\sigma_g$, $2\pi_u$ and $2\pi_g$ orbitals of Cl_2 from threshold to ~ 20 eV photoelectron energy obtained using Hartree–Fock photoelectron orbitals. These studies were motivated by recent $(2+1)$ resonance enhanced multiphoton ionization (REMPI) experiments via the $2\,^1\Pi_g\,(2\pi_g^3 4s\sigma_g)$ state which show strong non-Franck–Condon effects in the ion vibrational distribution suggesting that shape and/or autoionizing resonances may play a role near threshold. Previous single-photon experiments on the valence orbitals of Cl_2 do not give a consistent picture of these cross sections at low energies. Our results show that there is a shape resonance in the $k\pi_u$ continuum. However, preliminary studies show that these π_u cross sections have almost no dependence on internuclear distance and could not be the cause of non-Franck–Condon effects observed in the REMPI experiments.

I. INTRODUCTION

In recent resonance enhanced multiphoton ionization (REMPI) studies of molecular chlorine via the $2\,^1\Pi_g\,(2\pi_g^3 4s\sigma_g)$ state, Koenders *et al.*[1] found ion vibrational distributions which could not be explained by a simple Franck–Condon picture. Such large non-Franck–Condon effects have been observed in REMPI of other diatomic molecules[2–10] and have been seen to arise from several different mechanisms.[11] In the case of molecular chlorine, studies by Li *et al.*[12,13] show that Rydberg–valence interactions involving the $1\,^1\Pi_g\,(\pi_u \rightarrow \sigma_u)$ valence state[14] are small, suggesting that low energy shape and/or autoionizing resonances may play a role in producing these non-Franck–Condon effects. Single-photon ionization studies of the valence orbitals of molecular chlorine have been carried out by Carlson *et al.*,[15] but these studies were mainly concerned with the region around the Cooper minimum at 30 to 40 eV above threshold and did not extend to low photoelectron energies. More recently, Samson *et al.*[16] have obtained total ion cross sections beginning around the $2\pi_u$ ionization threshold. These cross sections differ in magnitude by about a factor of 2 from those of Carlson *et al.*,[15] but show the same general dependence on energy. van de Meer *et al.*[17] have measured the photoionization cross sections for the valence oribitals of Cl_2 at the HeI line (21.2 eV). These measurements differ significantly from those of Carlson *et al.*[15] and are in better agreement but still differ with the total ion cross sections of Samson *et al.*[16] To try to understand these differences and to provide some insight into how the electronic continuum may affect REMPI experiments on Cl_2, we have obtained photoionization cross sections and photoelectron asymmetry parameters for single-photon ionization of the valence orbitals $(5\sigma_g, 2\pi_u, 2\pi_g)$ of Cl_2 from threshold to ~ 20 eV photoelectron energy using Hartree–Fock photoelectron orbitals. These studies are preliminary to REMPI studies of Cl_2 via the $2\,^1\Pi_g$ state.

It is well known that interchannel coupling is important in $3p$ photoionization of chlorine atom at low photoelectron energies.[18–20] Such coupling can also be expected to be important in the photoionization of molecular chlorine. Nevertheless, the present study should illustrate some general dynamical features of the photoionization cross sections of Cl_2 and serve as a basis for future studies beyond the Hartree–Fock level. Indeed, we do find strong shape resonant structure in the $k\pi_u$ continuum which arises mainly from the $l=3$ partial wave, not unlike but more pronounced than that seen in F_2.[21] Preliminary studies indicate, however, that these cross sections do not depend on internuclear distance. These results suggest that a shape resonant mechanism is probably not responsible for the non-Franck–Condon effects observed in the REMPI experiments of Koenders *et al.*[1] and that other mechanisms need to be investigated.

In Sec. II we give a brief description of our procedure for obtaining the Hartree–Fock photoelectron oribitals. In Sec. III we present our photoionization cross sections and photoelectron asymmetry parameters for the $5\sigma_g, 2\pi_u$, and $2\pi_g$ orbitals of Cl_2 and compare these with experimental results.

II. METHOD AND CALCULATIONS

Our method for obtaining Hartree–Fock photoelectron orbitals has been discussed extensively elsewhere[22,23] and will only be briefly summarized here. We assume a frozen core Hartree–Fock model in which the ion orbitals are constrained to be identical to those of the neutral molecule and the photoelectron orbital is a solution of the one-electron Schrödinger equation

$$\left[-\frac{1}{2}\nabla^2 + V_{N-1}(\mathbf{r},R) - \frac{k^2}{2}\right]\phi_k(\mathbf{r},R) = 0, \qquad (1)$$

where $V_{N-1}(\mathbf{r},R)$ is the static-exchange potential of the molecular ion, $k^2/2$ is the photoelectron kinetic energy, and ϕ_k satisfies appropriate scattering boundary conditions. To solve for ϕ_k we work with the integral form of Eq. (1), i.e., the Lippmann–Schwinger equation

$$\phi_k = \phi_k^c + G_c^{(-)} V \phi_k, \qquad (2)$$

where ϕ_k^c is the Coulomb scattering wave function, V is the molecular ion potential V_{N-1} with the Coulomb potential removed, and $G_c^{(-)}$ is the Coulomb Green's function with incoming-wave boundary conditions. We first obtain an approximate solution of Eq. (2) by assuming a separable approximation to the potential V of the form

 0021-9606/90/084887-06$03.00

$$V(\mathbf{r},\mathbf{r}') \cong V^s(\mathbf{r},\mathbf{r}') = \sum_{i,j} \langle \mathbf{r}|V|\alpha_i\rangle [V^{-1}]_{ij} \langle \alpha_j|V|\mathbf{r}'\rangle, \tag{3}$$

where the matrix V^{-1} is the inverse of the matrix with elements $V_{ij} = \langle \alpha_i|V|\alpha_j\rangle$ and the α's are discrete basis functions such as Cartesian or spherical Gaussian functions.[22] With this approximation to V, the partial wave solution to the integral equation can be written as

$$\phi^{(0)}_{klm}(\mathbf{r}) = \phi^c_{klm}(\mathbf{r}) + \sum_{ij} \langle \mathbf{r}|G_c^{(-)}V|\alpha_i\rangle [D^{-1}]_{ij} \langle \alpha_j|V|\phi^c_{klm}\rangle, \tag{4}$$

where

$$D_{ij} = \langle \alpha_i|V - VG_c^{(-)}V|\alpha_j\rangle \tag{5}$$

and

$$\phi_{\mathbf{k}}(\mathbf{r}) = \left(\frac{2}{\pi}\right)^{1/2} \sum_{l=0}^{l_p} \sum_{m=-l}^{l} i^l \phi_{klm}(\mathbf{r}) Y^*_{lm}(\hat{\mathbf{k}}). \tag{6}$$

With adequate basis sets α's, these approximate solutions $\phi^{(0)}_{klm}$, which satisfy scattering boundary conditions, can provide quantitatively reliable cross sections[24] and have been used in calculating the photoionization cross sections and photoelectron asymmetry parameters reported below.

TABLE I. Basis sets used in separable potential, Eq. (3).

Photoionization symmetry	Type of Gaussian function[a]		Exponents
σ_g	Cartesian	s	16.0,8.0,4.0,2.0,1.0,0.5,0.1
		z	1.0,0.5,0.1
	Spherical	$l=0$	4.0,2.0,1.0,0.5,0.1
		$l=2$	4.0,2.0,1.0,0.5,0.1
		$l=4$	1.0,0.5,0.1
σ_u	Cartesian	s	16.0,8.0,4.0,2.0,1.0,0.5,0.1
		z	1.0,0.5,0.1
	Spherical	$l=1$	4.0,2.0,1.0,0.5,0.1
		$l=3$	4.0,2.0,1.0,0.5,0.1
		$l=5$	1.0,0.5,0.1
π_g	Cartesian	x	16.0,8.0,4.0,2.0,1.0,0.5,0.1
		xz	1.0,0.5,0.1
	Spherical	$l=2$	4.0,2.0,1.0,0.5,0.1
		$l=4$	4.0,2.0,1.0,0.5,0.1
π_u	Cartesian	x	16.0,8.0,4.0,2.0,1.0,0.5,0.1
		xz	1.0,0.5,0.1
	Spherical	$l=1$	4.0,2.0,1.0,0.5,0.1
		$l=3$	4.0,2.0,1.0,0.5,0.1
		$l=5$	1.0,0.5,0.1
δ_g	Cartesian	xy	16.0,8.0,4.0,2.0,1.0,0.5,0.1
	Spherical	$l=2$	4.0,2.0,1.0,0.5,0.1
		$l=4$	1.0,0.5,0.1
δ_u	Cartesian	xy	16.0,8.0,4.0,2.0,1.0,0.5,0.1
	Spherical	$l=3$	4.0,2.0,1.0,0.5,0.1
		$l=5$	1.0,0.5,0.1

[a] Cartesian Gaussian basis functions are defined as $\phi^{\alpha,l,m,n,\mathbf{A}}(\mathbf{r}) = N(x-A_x)^l(y-A_y)^m(z-A_z)^n \exp(-\alpha|\mathbf{r}-\mathbf{A}|^2)$ and spherical Gaussian functions as $\phi^{\alpha,l,m,\mathbf{A}}(\mathbf{r}) = N|\mathbf{r}-\mathbf{A}|^l \exp(-\alpha|\mathbf{r}-\mathbf{A}|^2) Y_{lm}(\Omega_{\mathbf{r}-\mathbf{A}})$. The Cartesian functions are centered on the nuclei and spherical functions on the bond midpoint.

For the ground state SCF wave function of Cl_2 with its electronic configuration $1\sigma_g^2 1\sigma_u^2 2\sigma_g^2 2\sigma_u^2 3\sigma_g^2 3\sigma_u^2 1\pi_u^4 1\pi_g^4 4\sigma_g^2 4\sigma_u^2 5\sigma_g^2 2\pi_u^4 2\pi_g^4$ we used the [8s5p] contracted Gaussian basis set of Dunning and Hay[25] with two additional d-type polarization functions with exponents 0.797 and 0.220 on each nucleus.[26] Calculations with this basis at the equilibrium geometry of Cl_2 ($R_e = 3.7568$ a.u.) give an SCF energy of $-918.908\,278$ a.u. For the basis sets $\{\alpha\}$ in Eqs. (3) and (4) we used Cartesian Gaussian functions centered on the atomic nuclei and spherical Gaussians at the center of mass. These functions for each photoelectron symmetry are given in Table I.

All matrix elements and functions arising in the solution of the Lippmann–Schwinger equation, Eq. (2), were evaluated via single-center expansions about the molecular center. The partial wave expansion of the photoelectron orbital, Eq. (6), was truncated at $l_p = 13$. The other partial wave expansion parameters were chosen as follows:

(i) maximum partial wave in the expansion of the occupied orbitals = 80,

(ii) maximum partial wave in the expansion of the occupied orbitals in the exchange potential = 80($1\sigma_g$),

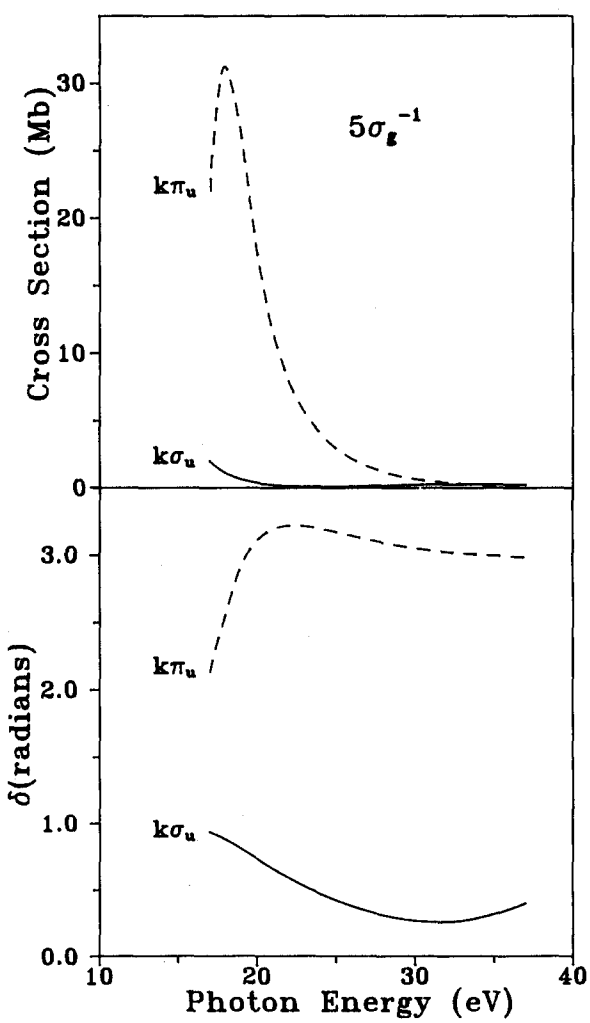

FIG. 1. Partial photoionization cross sections (length) and eigenphase sums for the $5\sigma_g$ orbital of Cl_2.

$80(1\sigma_u)$, $70(2\sigma_g)$, $70(2\sigma_u)$, $50(3\sigma_g)$, $50(3\sigma_u)$, $50(1\pi_u)$, $50(1\pi_g)$, $50(4\sigma_g)$, $50(4\sigma_u)$, $40(5\sigma_g)$, $40(2\pi_u)$, $40(2\pi_g)$,

(iii) maximum partial wave in the expansion of $1/r_{12}$ in the direct and exchange terms = 160 and 80, respectively,

(iv) all other partial wave expansions were truncated at $l = 80$.

Based on our studies with such partial-wave expansions, this choice of expansion parameters should provide cross sections within a few percent of the converged values. The associated radial integrals were obtained using a Simpson's rule quadrature. The grid contained 850 points and extended to 94.5 a.u.with a step size varying from 0.01 a.u. near the atomic nuclei to 0.5 a.u. at large distances.

III. RESULTS AND DISCUSSION

Figure 1 shows the $k\sigma_u$ and $k\pi_u$ partial cross sections and eigenphase sums for photoionization of the $5\sigma_g$ orbital of Cl_2, assuming an ionization potential (IP) of 16.1 eV.[27,28]

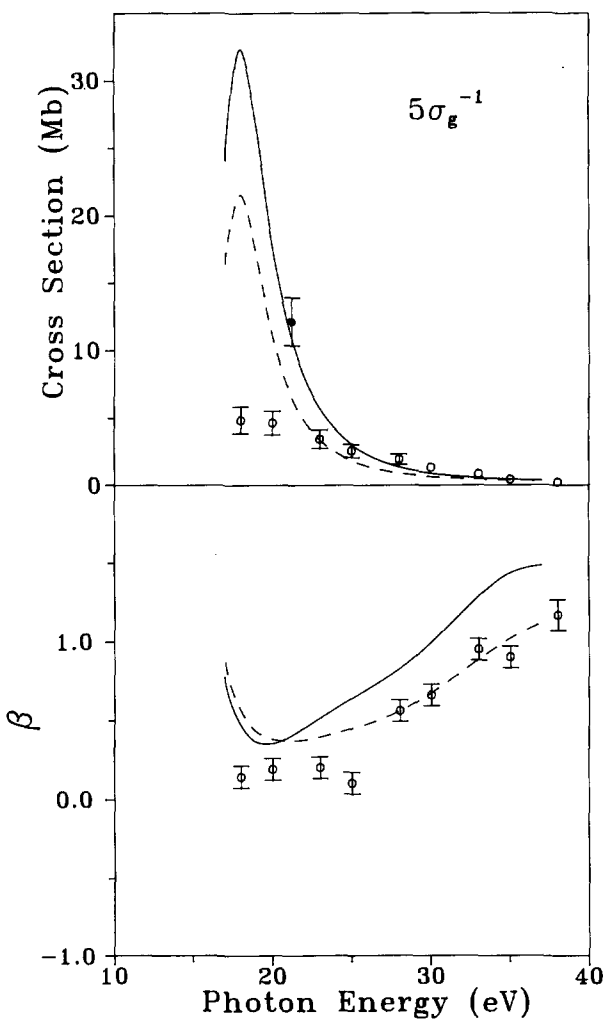

FIG. 2. Total photoionization cross sections and photoelectron asymmetry parameters for the $5\sigma_g$ orbital of Cl_2:—, present results (length);---, present results (velocity); O, synchrotron measurements of Ref. 15. Error bars are not shown at higher energies; ●, HeI line measurement of Ref. 17.

In contrast to what is seen in other lighter diatomics such as N_2 [29] and O_2 [30] with their shorter bond lengths, the $k\sigma_u$ channel is weak and shows no evidence of shape resonant behavior at these internuclear distances. The $k\pi_u$ eigenphase sum shows a rapid rise near threshold which is reflected in the large enhancement in the $k\pi_u$ partial channel cross section. Calculations at several internuclear distances show almost no change in these $k\pi_u$ cross sections, in contrast to previous studies of the behavior of $k\sigma_u$ shape resonances in other molecules.[31] For a $k\pi_u$ shape resonance, oriented perpendicular to the molecular axis, one perhaps would not expect changes in the bond length to affect the cross sections. With its insensitivity to bond distance, this shape resonant continuum *should not* lead to any significant non-Franck–Condon behavior.

Examination of the U matrix which diagonalizes the K matrix to obtain the eigenphase sum[32]

$$\delta = \sum_{lm} \arctan(U^{\dagger} K U) \tag{7}$$

shows this resonance behavior to be associated principally with the $l = 3$ partial wave. Indeed, a plot of the corresponding resonant eigenchannel function[32]

$$\psi_\alpha = \sum_{lm} \psi_{lm} U_{lm\,\alpha}, \tag{8}$$

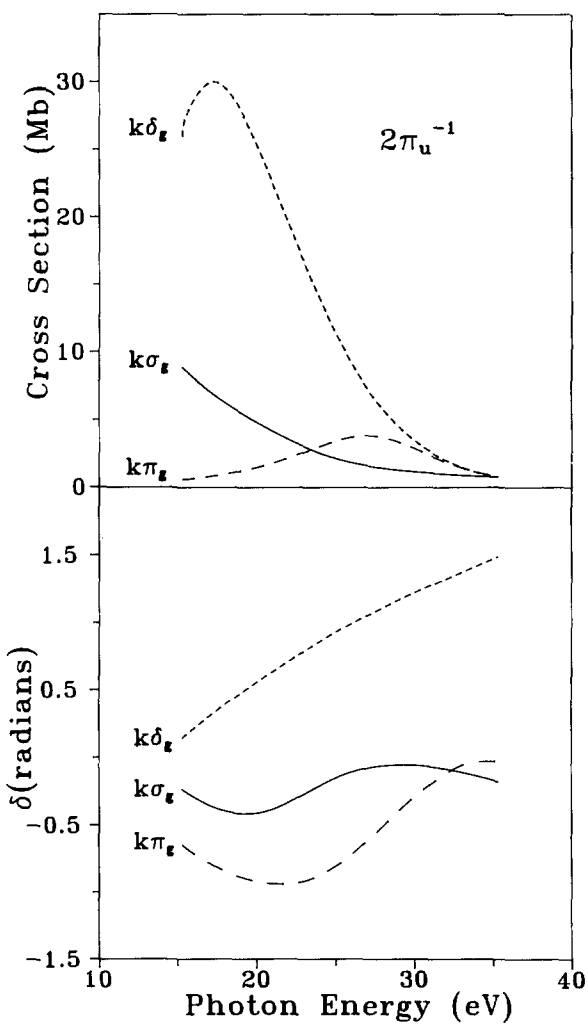

FIG. 3. Partial photoionization cross sections (length) and eigenphase sums for the $2\pi_u$ orbital of Cl_2.

where ψ_{lm} is the K-matrix normalized partial wave component of the continuum orbital and α is an eigenchannel index, shows f-wave nodal structure (not shown).

In Fig. 2 we show our calculated cross sections and photoelectron asymmetry parameters for photoionization of the $5\sigma_g$ orbital of Cl_2 along with the experimental synchrotron results of Carlson *et al.*[15] and the HeI line measurement of van der Meer *et al.*[17] Differences between the cross sections obtained in the length and velocity approximations are known to arise primarily from neglect of electronic correlations in the Hartree–Fock wave functions used here.[23] The pronounced peak in the calculated cross sections arises from the shape resonant $k\pi_u$ partial channel shown in Fig. 1. Below $\sim$25 eV photon energy there are large differences between the measured values of Carlson *et al.*[15] and the present results. The results of multiple-scattering model (MSM) calculations of Carlson *et al.*,[15] which extend down to $\sim$19 eV photon energy (not shown) agree well with the present calculations, showing the same enhancement near threshold. The agreement between the He I line measurement of van der Meer *et al.*[17] and the calculated cross sections is encouraging. Additional measurements at low photoelectron energies would be helpful in clarifying the resonant behavior of these cross sections. The agreement between the calculated photoelectron asymmetry parameters and the measurements of Carlson *et al.*[15] is also quite satisfactory. Further experimental studies of these asymmetry parameters in the region of the "dip" in the present results would be helpful.

Figure 3 shows our calculated partial cross sections and eigenphase sums for the $2\pi_u$ orbital of Cl_2 assuming an ionization potential of 14.4 eV.[27,28] The $k\delta_g$ cross section, which is primarily $l = 2$, shows a broad enhancement at low energy. The $k\pi_g$ cross section is small at low energy and shows a mild enhancement at $\sim$25 eV photon energy where the eigenphase sum rises slightly due to the $l = 4$ partial wave. The total cross sections and photoelectron asymmetry parameters for the $2\pi_u$ level are shown in Fig. 4. There are again substantial differences between the present calculated results and the measurements of Carlson *et al.*[15] The cross section at the HeI line measured by van der Meer *et al.*[17] is again also in good agreement with the calculated value. The calculated photoelectron angular distributions, however, agree well with the measurements of Carlson *et al.*[15] over the entire energy range.

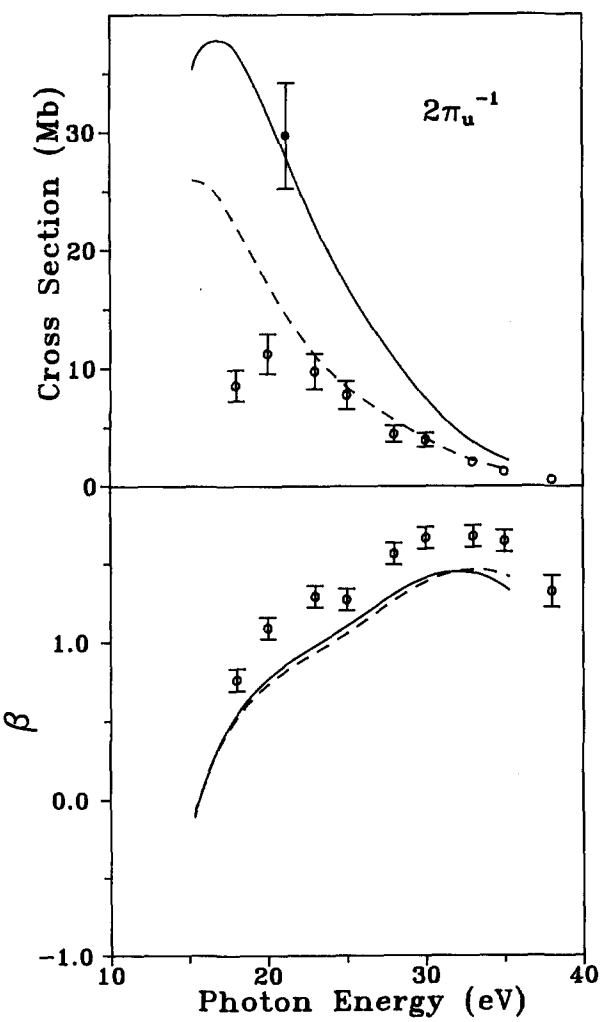

FIG. 4. Total photoionization cross sections and photoelectron asymmetry parameters for the $2\pi_u$ orbital of Cl_2:—, present results (length);---, present results (velocity); ○, synchrotron measurements of Ref. 15. Error bars are not shown at higher energies; ●, HeI line measurement of Ref. 17.

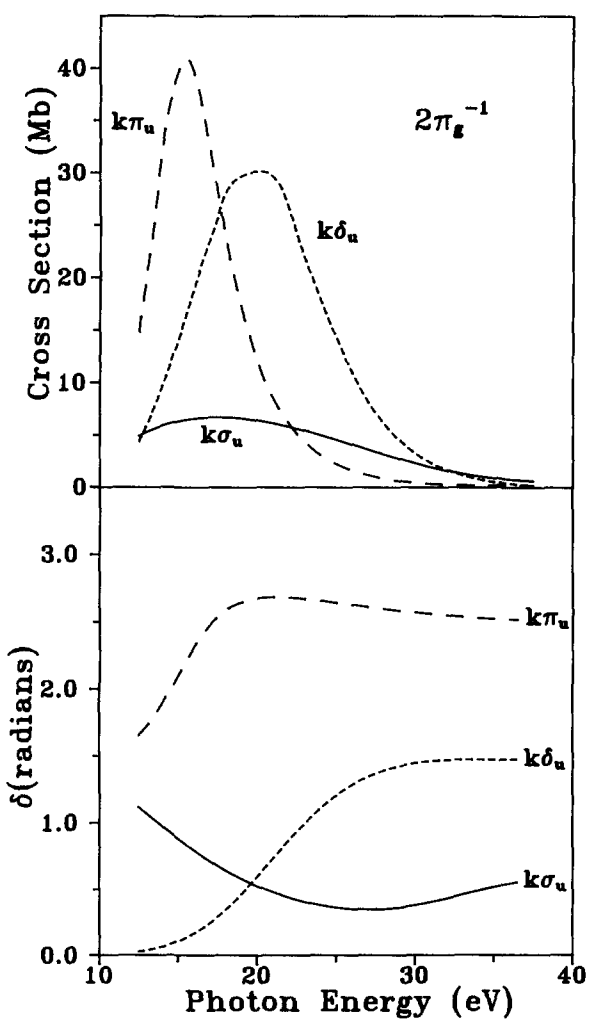

FIG. 5. Partial photoionization cross sections (length) and eigenphase sums for the $2\pi_g$ orbital of Cl_2.

In Fig. 5 we show the partial cross sections and eigenphase sums for photoionization of the $2\pi_g$ level (IP = 11.6 eV).[27,28] The $k\pi_u$ eigenphase sums show the same rise near threshold seen in $5\sigma_g$ photoionization. There is a similar but slow rise in the $k\delta_u$ eigenphase sums. This behavior in the eigenphase sums is also evident in enhancements in the $k\pi_u$ and $k\delta_u$ cross sections. Figure 6 shows the total cross sections and photoelectron asymmetry parameters for $2\pi_g$ photoionization. Our calculated cross sections agree with those of Carlson *et al.*[15] above ~25 eV photon energy, but differ significantly closer to threshold. The agreement between the calculated cross sections and the measured value of van der Meer *et al.*[17] at the HeI line is again encouraging. The calculated photoelectron asymmetry parameters are in good agreement with the measured values of Carlson *et al.*[15]

Figure 7 shows the total photoionization cross sections for the $5\sigma_g + 2\pi_u + 2\pi_g$ orbitals of molecular chlorine along with results of experiment. The "steps" at low energy in the present results indicate the onset of these ionization thresholds. These thresholds are also indicated by the arrows on the photon energy axis. Note that the data of Samson *et al.*[16] record the total ion yield and include contributions from the $4\sigma_u$ orbital (IP~27 eV) and $4\sigma_g$ orbital (IP~34 eV). The data of Carlson *et al.*[15] and Samson *et al.*[16] show the same general energy dependence, except for the data point of Carlson *et al.*[16] at 18 eV photon energy, but differ substantially in magnitude. Above ~20 eV photon energy the data of Samson *et al.*[16] agree well with the present results. Below the $5\sigma_g$ threshold, however, the data of Samson *et al.*[16] and the present results show a quite different energy dependence. Several studies[33–35] show rich autoionizing structure within a few electron volts of the $2\pi_g$ ionization threshold and this may account for some of these differences. The data of van der Meer *et al.*[17] at 21.2 eV differs from that of Samson *et al.*[16] Both of these experimental results are bracketed by the present length and velocity Hartree–Fock results. The difference between the length and velocity results indicates that electron correlations beyond the Hartree–Fock level are important in this region. Future theoretical studies need to include such effects and interchannel coupling to understand these experimental cross sections. In addition, further experimental studies of orbital cross sections are needed to provide a consistent picture of photoionization of Cl_2 at low energies.

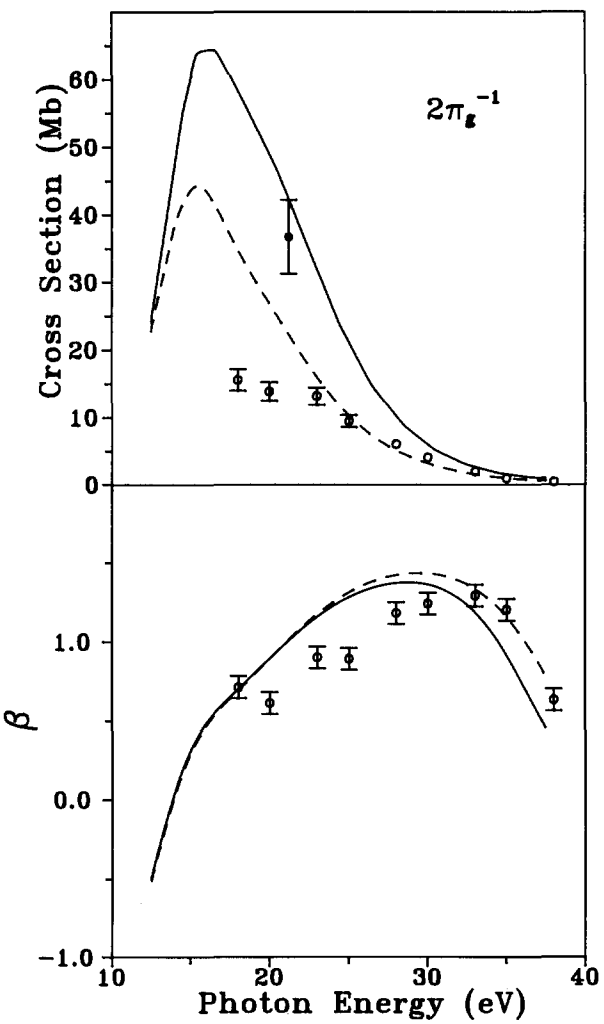

FIG. 6. Total photoionization cross sections and photoelectron asymmetry parameters for the $2\pi_g$ orbital of Cl_2:—, present results (length);---, present results (velocity); O, synchrotron measurements of Ref. 15. Error bars are not shown at higher energies; ●, HeI line measurement of Ref. 17.

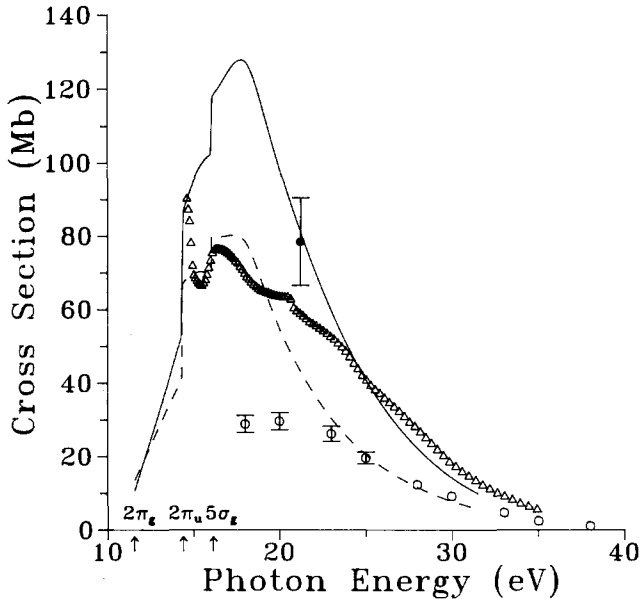

FIG. 7. Total photoionization cross sections ($5\sigma_g + 2\pi_u + 2\pi_g$) for Cl_2:—, present results (length);---, present results (velocity); O, synchrotron measurements of Ref. 15. Error bars are not shown at higher energies; ●, HeI line measurement of Ref. 17; Δ experimental measurements of Ref. 16. Above ~27 eV the data of Ref. 16 contain contributions from other lower lying molecular orbitals.

ACKNOWLEDGMENTS

This work was supported by a grant from the National Science Foundation (CHE-8521391). We also acknowledge use of resources of the San Diego SuperComputer Center, which is supported by the National Science Foundation, and the Air Force SuperComputer Center-Kirtland. One of us (M.B.) would like to acknowledge support from a Department of Education Graduate Fellowship and would also like to thank Dr. J. A. Stephens for providing data on atomic chlorine phase shifts.

[1]B. G. Koenders, S. M. Koeckhoven, G. J. Kuik, K. E. Drabe, and C. A. de Lange, J. Chem. Phys. **91**, 6042 (1989).
[2]M. G. White, M. Seaver, W. A. Chupka, and S. D. Colson, Phys. Rev. Lett. **49**, 28 (1982).
[3]M. G. White, M. Seaver, W. A. Chupka, and S. D. Colson, J. Chem. Phys. **80**, 678 (1984).
[4]J. C. Miller and R. N. Compton, J. Chem. Phys. **84**, 675 (1986).
[5]S. T. Pratt, P. M. Dehmer, and J. L. Dehmer, Chem. Phys. Lett. **105**, 28 (1984).
[6]S. T. Pratt, P. M. Dehmer, and J. L. Dehmer, J. Chem. Phys. **85**, 3379 (1986).
[7]S. Katsumata, K. Sato, Y. Achiba, and K. Kimura, J. Electron Spectrosc. Relat. Phenom. **41**, 325 (1986).
[8]P. J. Miller, L. Li, W. A. Chupka, and S. D. Colson, J. Chem. Phys. **89**, 3921 (1988).
[9]J. A. Stephens, M. Braunstein, and V. McKoy, J. Chem. Phys. **89**, 3923 (1988).
[10]M. Braunstein, J. A. Stephens, and V. McKoy, J. Chem. Phys. **90**, 633 (1989).
[11]See, for example, W. A. Chupka, J. Chem. Phys. **87**, 1488 (1987).
[12]L. Li, R. Lipert, H. Park, W. A. Chupka, and S. D. Colson, J. Chem. Phys. **87**, 6767 (1987).
[13]L. Li, R. Lipert, H. Park, W. A. Chupka, and S. D. Colson, J. Chem. Phys. **88**, 4608 (1988).
[14]S. D. Peyerimhoff and R. J. Buenker, Chem. Phys. **57**, 279 (1981).
[15]T. A. Carlson, M. O. Krause, F. A. Grimm, and T. A. Whitley, J. Chem. Phys. **78**, 638 (1983).
[16]J. A. R. Samson and G. C. Angel, J. Chem. Phys. **86**, 1814 (1987).
[17]W. J. van der Meer, R. J. Butselaar, and C. A. de Lange, Aust. J. Phys. **39**, 779 (1986).
[18]E. R. Brown, S. L. Carter, and H. P. Kelly, Phys. Rev. A **21**, 1237 (1980).
[19]W. R. Fielder and L. A. Armstrong, Jr., Phys. Rev. A **28**, 218 (1983).
[20]J. A. R. Samson, Y. Shefer, and G. C. Angel, Phys. Rev. Lett. **56**, 2020 (1986).
[21]A. E. Orel, T. N. Rescigno, B. V. McKoy, and P. W. Langhoff, J. Chem. Phys. **72**, 1265 (1980).
[22]R. R. Lucchese, G. Raseev, and V. McKoy, Phys. Rev. A **25**, 2572 (1982).
[23]R. R. Lucchese, K. Takatsuka, and V. McKoy, Phys. Rep. **131**, 147 (1986).
[24]M. Braunstein and V. McKoy, J. Chem. Phys. **87**, 224 (1987).
[25]T. H. Dunning and P. J. Hay, in *Modern Theoretical Chemistry*, edited by H. F. Schaefer III (Plenum, New York, 1976), Vol. 3, Chap. 1.
[26]J. Andzelm, M. Klobukowski, E. Radzio-Andzelm, Y. Sakai, and H. Tatewaki, in *Gaussian Basis Sets for Molecular Calculations*, edited by S. Huzinaga (Elsevier, Amsterdam, 1984).
[27]A. B. Cornford, D. C. Frost, C. A. McDowell, J. L. Ragle,. and I. A. Stenhouse, J. Chem. Phys. **54**, 2651 (1971).
[28]A. W. Potts and W. C. Price, Trans. Faraday Soc. **67**, 1242 (1971).
[29]J. L. Dehmer and D. Dill, J. Chem. Phys. **65**, 5327 (1976); G. Raseev, H. Le Rouzo, and H. Lefebvre-Brion, *ibid.* **72**, 5701 (1980).
[30]A. Gerwer, C. Asaro, B. V. McKoy, and P. W. Langhoff, J. Chem. Phys. **72**, 713 (1980); P. M. Dittman, D. Dill, and J. L. Dehmer, *ibid.* **76**, 5703 (1982); T. Gustafsson, Chem. Phys. Lett. **75**, 505 (1980).
[31]See, for example, J. L. Dehmer, A. C. Parr, and S. H. Southworth, in *Handbook on Synchrotron Radiation*, edited by G. V. Marr (North-Holland, Amsterdam, 1986), Vol. II.
[32]D. Loomba, S. Wallace, and D. Dill, J. Chem. Phys. **75**, 4546 (1981).
[33]V. H. Dibeler, J. A. Walker, K. E. McCulloh, and H. M. Rosenstock, Int. J. Mass Spectrom. Ion Phys. **7**, 209 (1971).
[34]R. J. Stubbs, T. A. York, and J. Comer, J. Phys. B **18**, 3229 (1985).
[35]J. Berkowitz, C. A. Mayhew, and B. Ruscic, Chem. Phys. **123**, 317 (1988).